**JURNAL PENELITIAN GEOGRAFI**
Vol (13), No (**2**), (2025), pp. 187-206
Doi: http://dx.doi.org/10.23960/jpg

**Original Article**

# Spatial Distribution Analysis of Land Use, Land Surface Temperature, and Temperature-Humidity Index in Bogor City in 2004, 2014, and 2024

**Ridho Gustiawan[1*] , Erwin Hermawan[1] , Nurul Kamilah[1] , Dewi Primasari[1]**

[1]Department of Computer Science, Faculty of Engineering & Science, Ibn Khaldun University Bogor, Bogor City, Indonesia

*Corresponding Email: rdhgstwnn18@gmail.com

**ABSTRACT**
Rapid urbanization in Bogor City in 2004, 2014, and 2024 caused significant changes in land use, marked by an increase in built-up areas and a decrease in vegetation cover. These changes triggered an increase in Land Surface Temperature (LST) and Temperature Humidity Index (THI), which had an impact on heat stress, health disorders, and a decline in quality of life. This study analyzes the relationship between land use changes and LST and THI and develops an interactive web application for visualization. Land classification was performed using the Random Forest algorithm, LST was calculated from Landsat thermal bands (TM 2004, OLI/TIRS 2014 & 2024), and THI was based on Air Temperature ($T_{(a)}$ )and Relative Humidity (RH). The results show that built-up land increased by 2,074 ha (from 4,371 ha to 6,445 ha), in line with an increase in average LST from 26.16°C to 27.13°C and THI from 24.30 to 24.90. In conclusion, the increase in built-up area contributed significantly to the rise in LST and THI, emphasizing the importance of sustainable spatial planning, such as optimizing green open spaces to maintain thermal comfort and quality of life.

**KEYWORDS**
Land Use; Surface Temperature; Air Temperature; Air Humidity; Thermal Comfort Level

**Received**: July 7, 2025 **Acepted**: July 29, 2025 **Published**: September 30, 2025

**Citation:**
Gustiawan, R., Hermawan, E., Kamilah, N., & Primasari, D. (2025). Spatial Distribution Analysis of Land Use, Land Surface Temperature, and Temperature-Humidity Index in Bogor City in 2004, 2014, and 2024. *Jurnal Penelitian Geografi*, *13*(2), 187–206. https://doi.org/10.23960/jpg.v13.i2.33610



## INTRODUCTION

Major cities in Indonesia, especially on the island of Java, face rapid population growth, with projections reaching 281.6 million by 2024. Java, which covers only 7% of Indonesia's territory, is home to about 56% of the national population**.** One city experiencing significant growth is Bogor, with a projected population of 1.5 million by 2024 (BPS, 2025). Its strategic location has made Bogor City a major destination for urbanization in West Java, especially during the 2011–2019 period. This urbanization has

driven rapid development, leading to the expansion of settlements and infrastructure, reducing agricultural land, and decreasing vegetation cover as built-up areas expand (Reja, Riyadi, & Mujiati, 2020).

Land use is the result of a complex interaction between social, economic, and environmental factors that influence how humans utilize the earth's surface for various activities such as agriculture, settlements, and industry. Changes in land use, particularly the reduction of vegetation, have resulted in a decline in *the Normalized Difference Vegetation Index* (NDVI) (Prasad, Ray, & Justice, 2022). NDVI is an indicator used to assess the level of greenness or the amount of vegetation in an area (Insan & Prasetya, 2021). NDVI values range from -1 to 1, where values close to 1 indicate healthy and dense vegetation, while values close to 0 or negative indicate non-vegetation areas such as water, open land, or clouds (Yengoh, Dent, Olsson, Tengberg, & Tucker III, 2016).

The decline in vegetation in urban areas contributes to an increase in *land surface temperature* (LST) and a decrease in *relative* humidity (RH). The combination of increased temperature and decreased humidity has an impact on the rise of *the Temperature Humidity Index* (THI), a thermal comfort indicator that represents heat stress on humans. A biometeorological approach shows that changes in atmospheric components such as temperature and humidity have a significant effect on human thermal balance and environmental comfort levels (Ebi, Burton, & McGregor, 2009). LST can be analyzed through satellite observations and meteorological station data, where remote sensing techniques play an important role in mapping temperature trends and identifying long-term climate change (Hansen, Ruedy, Sato, & Lo, 2010). In general, surface temperature is defined as the skin temperature of the earth's surface. In open areas, surface temperature is the temperature of the ground, while in areas with high vegetation density, surface temperature is the temperature of the vegetation canopy (Erkamim et al., 2023) .

THI is an indicator that combines surface temperature (*Air* Temperature/$T_a$ ) and RH to assess the level of comfort or heat stress in humans, animals, and plants. THI is measured in degrees Celsius and relates to the thermal comfort of human populations in urban areas (Effendy, 2007). *Air Temperature* is a measure of the heat or coldness of the atmosphere measured at a certain height above the earth's surface, usually 1.5 to 2 meters. Air temperature is determined by the movement of air molecules; the faster they move, the higher the measured temperature (Spiridonov & Ćurić, 2021). Temperature measurements usually use *the Celsius* (C), *Reamur* (R), and Fahrenheit (F) scales (Winarno, Harianto, & Santoso, 2019). RH is the amount of water vapor contained in the air and can be measured with *a hygrometer*. RH is a common indicator of water vapor content in the atmosphere because it is easy to measure and understand. When RH reaches 100%, the air is saturated and condensation occurs, forming clouds, fog, or dew. RH also affects the thermal comfort of humans and animals because high humidity reduces the effectiveness of body cooling through sweat evaporation (Jing, Li, Tan, & Liu, 2013).

In the long term, increases in LST and THI can cause serious impacts such as heat stress, health disorders, reduced air quality, and a decline in the quality of life of urban communities (Damayanti, Safe'i, Setiawan, & Yuwono, 2023). THI is an important tool for measuring environmental comfort levels and identifying conditions that affect human physical and mental well-being (Fauzi, Kharisudin, Wasono, Utami, & Harmoko, 2023). If temperature and humidity are within the ideal range, the human body can achieve thermal equilibrium, allowing daily activities to be carried out comfortably, efficiently, and productively (Azahra & Kartikawati, 2021).

The Google Earth Engine (GEE)-based remote sensing approach is used to analyze satellite images quickly, accurately, and extensively with *JavaScript* or *Python* programming languages *(Samsu Rijal, 2020)*. These scripts are run through Earth Engine Code Editor, a web-based integrated development environment that makes it easy for users to write, run, and save code (Cardille, Crowley, Saah, & Clinton, 2024). Remote sensing is a technology for analyzing the Earth's surface from a distance, with recording done in the air or in space using sensors and vehicles (Yanuarsyah, Susetyo, Hermawan, & Hudjimartsu, 2025).

This technology enables effective spatial mapping, which is an important part of non-structural mitigation strategies and is relevant in supporting environmental policy planning, particularly in the city of Bogor through LST and THI analysis (Ita Selvia, Virgota, Arifin Aria Bakti, Sukartono, & Hari Kusumo, 2025). One study noted an increase in built-up land of 87.49 ha in 10 years, accompanied by an increase in LST of up to 5°C and THI of 3°C (Baihaqi, Prasetyo, & Bashit, 2020). Built-up land was recorded as having the highest average temperature (27.18°C), while vegetation areas had the lowest temperature. Vegetation areas effectively reduce temperatures through evaporation and transpiration,

while the conversion of green areas triggers the risk of *the Urban Heat Island* (UHI) effect (Noviani, Saputra, Wijayanti, & Koesoma, 2024).

*The Random Forest* (RF) classification method based on satellite imagery on the GEE platform is used to accurately detect land use changes. *Random Forest* is a *machine learning* algorithm that forms a number of *decision trees* and combines the results to improve classification accuracy (Raharjo, 2022). Based on previous research, *Random Forest* has proven to be superior in accuracy, reaching 89.53%, much higher than *Support Vector Machine* (SVM) which is only 74.07% when applied to Landsat 8 images (Sheykhmousa et al., 2020).

Based on these issues, an analysis of the spatial distribution patterns of land use, *Land Surface Temperature*, and *Temperature Humidity Index* in Bogor City in 2004, 2014, and 2024 is needed. The year 2024 was chosen as the main focus of the analysis because it reflects the current conditions after a decade of rapid urbanization. By comparing data from 2004, 2014, and 2024, this study aims to reveal the dynamics of long-term changes in Bogor City. The results of this analysis are expected to provide in-depth insights into the spatial distribution of land changes, increases in LST, and THI, which can be used as a basis for mitigation strategies and urban planning that are responsive to the impacts of climate change.

## METHOD

### Research Location

This research was conducted in Bogor City, and data processing was carried out at the *Geospatial Information Technology* (GIT) Laboratory, Department of Informatics Engineering, Ibn Khaldun University, Bogor. Geographically, Bogor City is located between 106º48' E and 6º26' S. The following is the research location map attached in Figure 1.

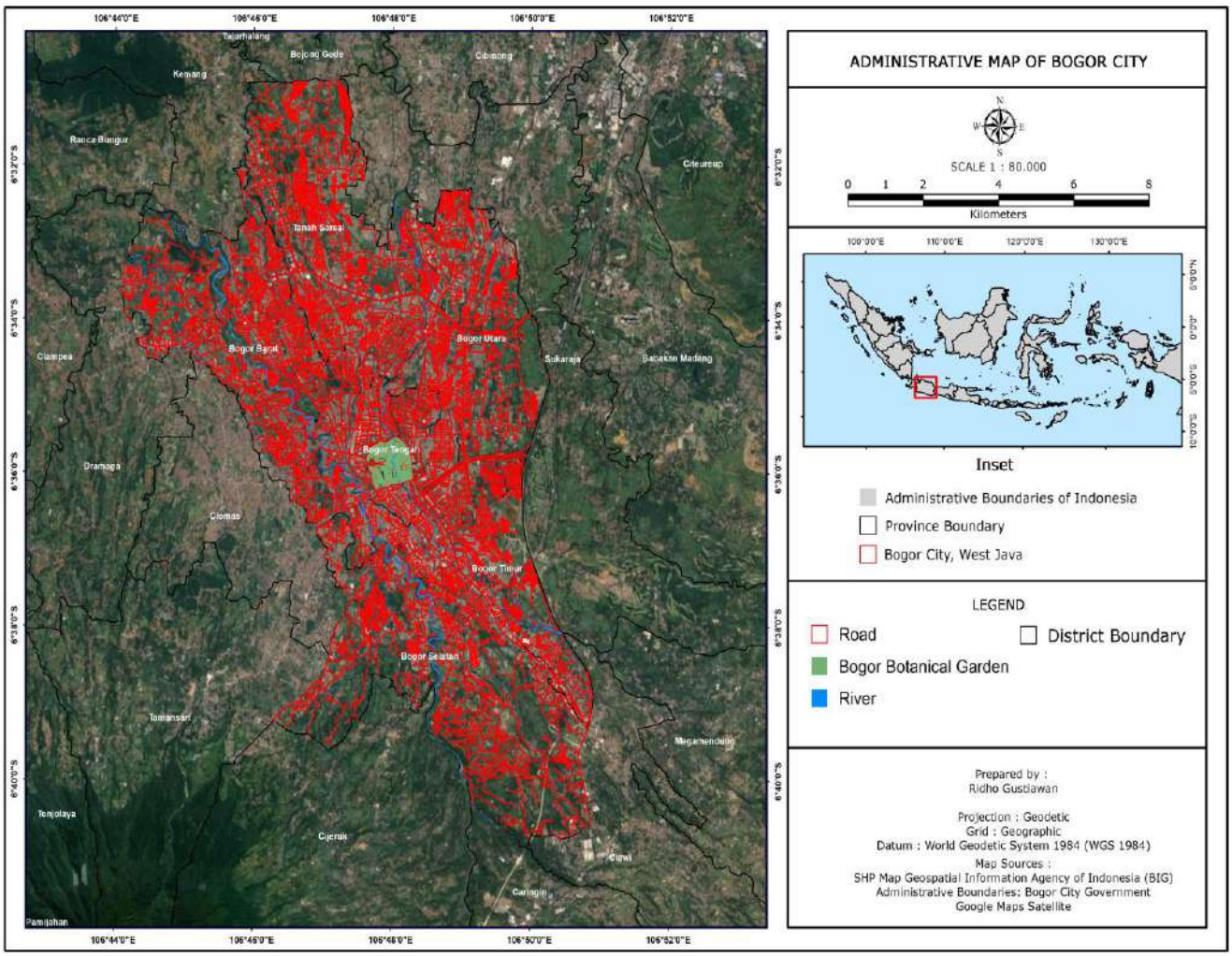


**Figure 1.** Research Location Map

**Research Procedures**

This research consists of three main stages: data collection, data processing and analysis, and web application development. Data collection was carried out at the beginning to obtain primary and secondary data from various sources. The processing and analysis stage included image filtering and cropping, land use processing, *Land Surface Temperature (*LST), *Air Temperature* Estimation *(*$T_{(a)}$ ), *Relative Humidity* Estimation *(*RH), and *Temperature Humidity Index* (THI) calculations. The final stage involves the development of a *Google Earth Engine (*GEE)*-based* web application to display the analysis results in the form of thematic maps, trend graphs, and spatial distributions to facilitate understanding of environmental changes and their impact on thermal comfort in the city of Bogor. The research flowchart is shown in Figure 2.

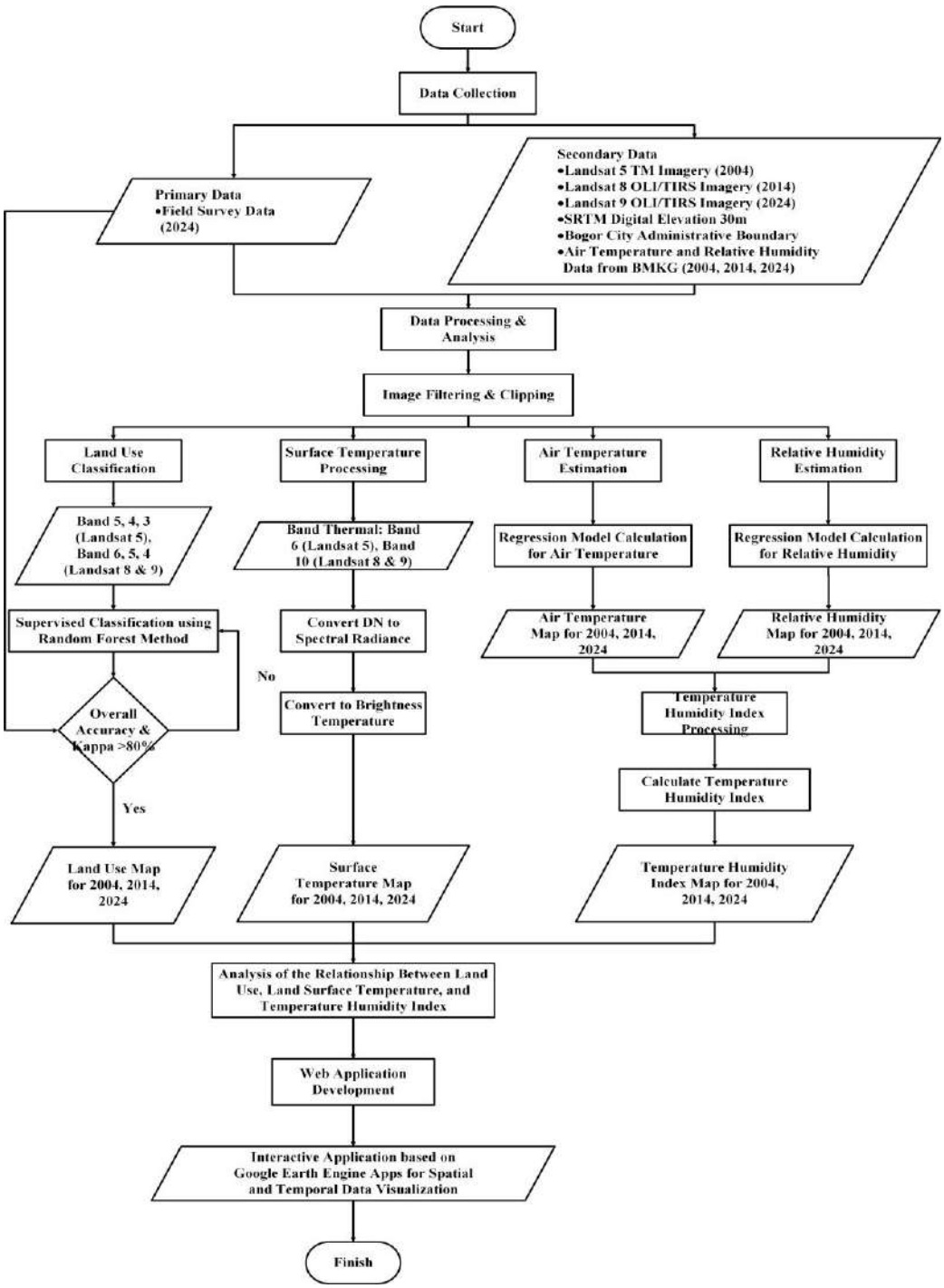


**Figure 2.** Flowchart

**Data Collection Instruments**

The researchers collected two main types of data, namely primary and secondary data, which formed the basis of this study's analysis.

a. Primary data

was obtained through field surveys at 131 strategic points in the Bogor City area, which focused on verifying land use conditions in the field. These points represent seven land use classifications, namely water bodies, built-up land, rice fields, gardens, forests, open land, and shrubs.

b. The secondary data

used consists of Landsat 5 TM satellite imagery (2004), Landsat 8 OLI/TIRS (2014), and Landsat 9 OLI/TIRS (2024), which were processed using the *Google Earth Engine* (GEE) platform to obtain information on land use, *Land Surface Temperature* (LST), and *Normalized Difference Vegetation Index* (NDVI). In addition, the researchers also used *Digital Elevation Model* (DEM) data with a resolution of 30 meters to support topographic analysis, as well as daily *Air Temperature* ($T_{a)}$ )and *Relative Humidity* (RH) data from the BMKG station in Bogor City to support the calculation of *the Temperature Humidity Index* (THI).

**Data Analysis**

The entire data processing and analysis process was carried out in an integrated manner on the *Google Earth Engine* (GEE) platform, using Landsat 5, 8, and 9 images. The stages carried out included:

a. Image Filtering and Cropping

Images were filtered based on year (2004, 2014, 2024) and *cloud cover* <20% using *filterDate()* and *filterMetadata()*. The images were then clipped according to the administrative boundaries of Bogor City using *clip()* with a shapefile of the region.

b. Land use classification

Image processing was performed using band composites (4-3-2 for Landsat 5, 6-5-4 for Landsat 8/9), then classified using the *Supervised Classification* method with the *Random Forest* (RF) algorithm. The model training process was performed using *.train()* and classification using *.classify()* (M, Ahmed, & N, 2023). The classification results were divided into seven land use classes: water bodies, built-up areas, gardens, rice fields, forests, open land, and shrubs.

c. Land Use Accuracy Test

Accuracy was evaluated by comparing the classification results with reference data from high-resolution imagery and field observations. Accuracy was calculated, and the classification results were considered valid if the *Overall Accuracy* value was ≥ 80% (Congalton & Green, 2008). Kappa accuracy can be expressed using formula (1) as follows:

$$Produscer\ Accuracy = \frac{Total\ number\ of\ correct\ land\ classes}{Total\ number\ of\ land\ class\ columns} \times 100\%$$

$$User\ Accuracy = \frac{Total\ number\ of\ land\ classes}{Total\ number\ of\ land\ class\ rows} \times 100\%$$

$$Overall\ Accuracy = \frac{Total\ number\ of\ correct\ classifications}{Total\ number\ of\ classifications} \times 100\%$$

$$Koefisien\ Kappa = \frac{N\ \sum_{k-1}^{r} X_{kk} - \sum_{k-1}^{r}(X_{k+} \times X_{+k})}{N^2 - \sum_{k-1}^{r}(X_{k+} \times X_{+k})}$$

$$Koefisien\ Kappa = \frac{N^A\ -\ B}{N^2\ -\ B} \times 100 \quad (1)$$

d. *Land Surface Temperature* Processing

*Land Surface Temperature* (LST) is calculated from thermal images (Band 6 for Landsat 5 and Band 10 for Landsat 8/9). The process begins with the conversion of *Digital Number* (DN) to *spectral radiance*, then brightness temperature, and finally LST (Nugroho, Wijaya, & Sukmono, 2016). LST calculations refer to Equation (2) and Equation (3) in GEE. The LST calculation stages are carried out through two main processes:

Conversion of *Digital Number* (DN) to Spectral Radiant

$$L\ =\ M_L\ \cdot DN\ +\ A_L \quad (2)$$

Conversion of *Spectral Radian* to Brightness Temperature and *Land Surface Temperature*

$$LST\ = \frac{K_2}{In(\frac{K_1}{L_\lambda} + 1)} -\ 273.15 \quad (3)$$

e. *Air Temperature* Estimation

*Air temperature* ($T_a$) estimation was performed using multiple linear regression (Zhang, Zhang, Ye, Che, & Zhang, 2016) between LST and DEM against BMKG temperature data, using the *Ordinary Least Squares* (OLS) method in Excel. The average LST and DEM values were obtained from a fishnet grid constructed in ArcGIS.

Multiple linear regression is a statistical method used to explain the relationship between one dependent variable and two or more independent variables in the form of a linear equation (Susetyo, 2010). The general equation for this method is shown in equation (4) as

follows:

$$Y = B_0 + B_1X_1 + B_2X_2 + \ldots + B_kX_k \quad (4)$$

The multiple regression model was then applied spatially in GEE using equation (5) below:

$$T_a = Y + (X_1 \cdot LST) + (X_2 \cdot DEM) \quad (5)$$

f. *Relative Humidity* Estimation

The process of estimating air humidity or *Relative Humidity* (RH) was carried out using a similar approach, using LST and NDVI as predictor variables and RH data from BMKG as the response. The average values of LST and NDVI were extracted from the same grid, and the analysis was performed using OLS. NDVI was calculated using the Near Infrared (NIR) and Red bands from Landsat images based on equation (6) (Hardjo & Susila, 2025).

$$NDVI = \frac{\text{NIR} - \text{Red}}{\text{NIR} + \text{Red}} \quad (6)$$

The model was applied in GEE using equation (7).

$$RH = Y + (X_1 \cdot LST) + (X_2 \cdot NDVI) \quad (7)$$

g. *Temperature Humidity Index* Processing

*The Temperature Humidity Index* (THI) is calculated to evaluate thermal comfort based on estimated air temperature and RH. This calculation uses a formula from Nieuwolt (1975) modified by Effendy (2007). The THI calculation formula used is shown in equation (8).

$$THI = 0.8Ta + \frac{RH + Ta}{500} \quad (8)$$

The THI value obtained is then classified into four categories of thermal comfort zones, as shown in Table 1.

**Table 1.** *Temperature Humidity Index* Values

| THI Value Range | Description |
|---|---|
| < 20 | Uncomfortable (Too cool) |
| 20 to 24 | Comfortable |
| 24 to 26 | Fairly comfortable |
| > 26 | Uncomfortable (Too hot) |

Source: Emmanuel R (2005) and Tursilowati L (2015)

**Analysis of the Relationship between Land Use, *Land Surface Temperature,* and *Temperature Humidity Index***

The analysis of the relationship between land use, *Land Surface Temperature* (LST), and *Temperature Humidity Index* (THI) aims to evaluate the impact of urbanization on temperature increases and thermal discomfort in the city of Bogor. The main focus of the analysis is to assess the contribution of built-up land expansion to increases in LST NDVI, $T_a$ , RH, and THI. The results are visualized in a combination graph.

**Web Application Development**

An interactive web application was developed using *Google Earth Engine Apps* through a series *of JavaScript-based* interface development stages. The initial stage included the design *of the panel UI* (such as buttons, *dropdowns*, and separate maps). Next, the application presented thematic maps of the spatial analysis results displaying the parameters. Users could select specific years and parameters through the interface controls provided. The application also features temporal trend graphs that enable interactive exploration of environmental dynamics (Wu, 2024).

## RESULTS AND DISCUSSION

**Image Filtering & Cropping**

This process begins with *filtering*, which is the process of filtering images based on cloud cover levels below a certain threshold in order to eliminate *pixels* affected by clouds or cloud shadows that can interfere with the accuracy of the analysis results. After the images are filtered, *clipping* is performed based on the administrative boundaries of the city of Bogor using a predetermined *shapefile*. This process aims to limit the analysis area to only the relevant study area.

**Land Use Classification**

The classification map displays the distribution of seven land use classes: water bodies, built-up land, gardens, rice fields, forests, open land, and shrubs. This visualization shows the dynamics of land use changes in line with the city's growth. The land use change map is shown in Figure 3, and the land use graphs for 2004, 2014, and 2024 are shown in Figure 4.

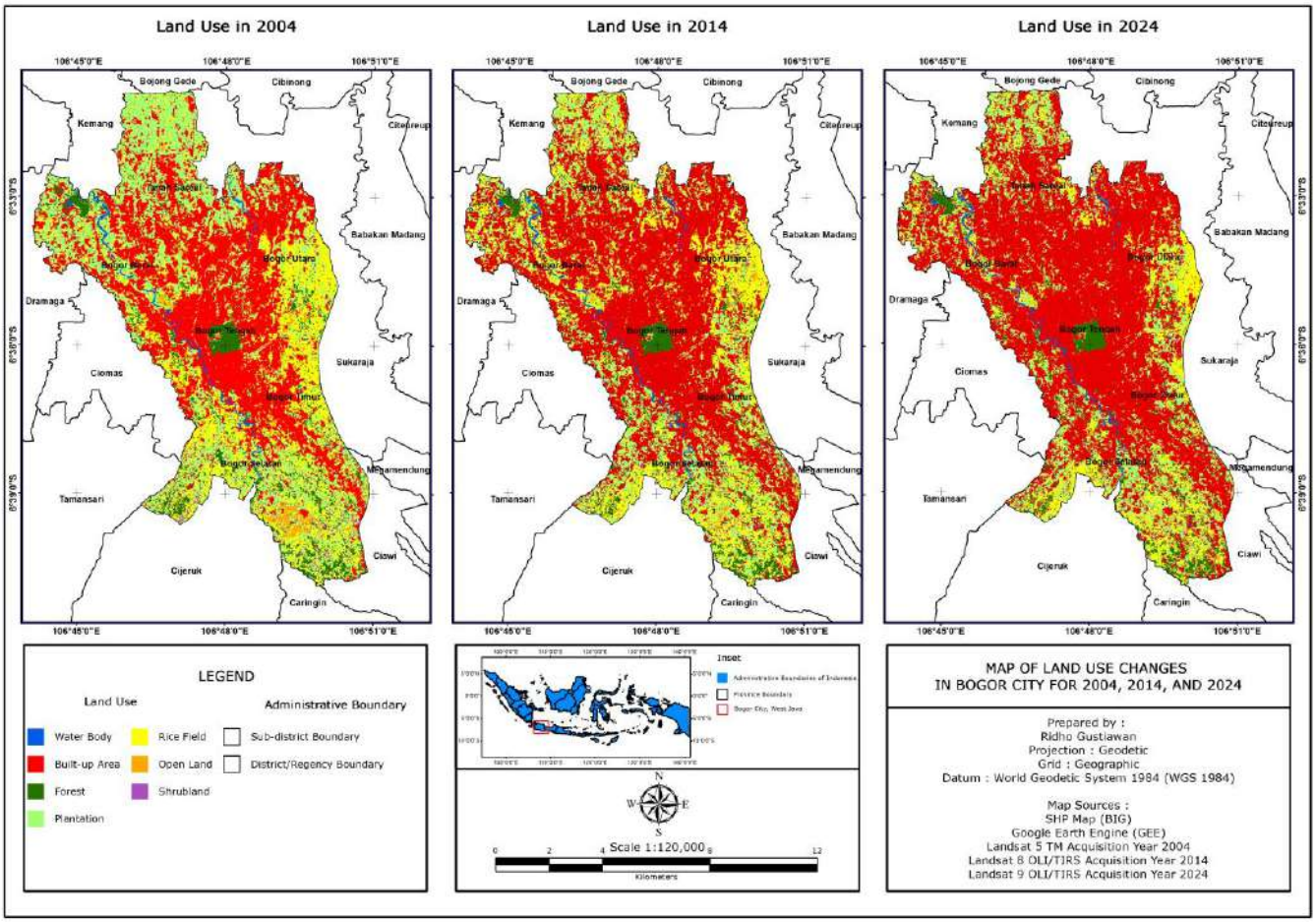


**Figure 3 .** Map of Land Use Change Areas for 2004, 2014, and 2024

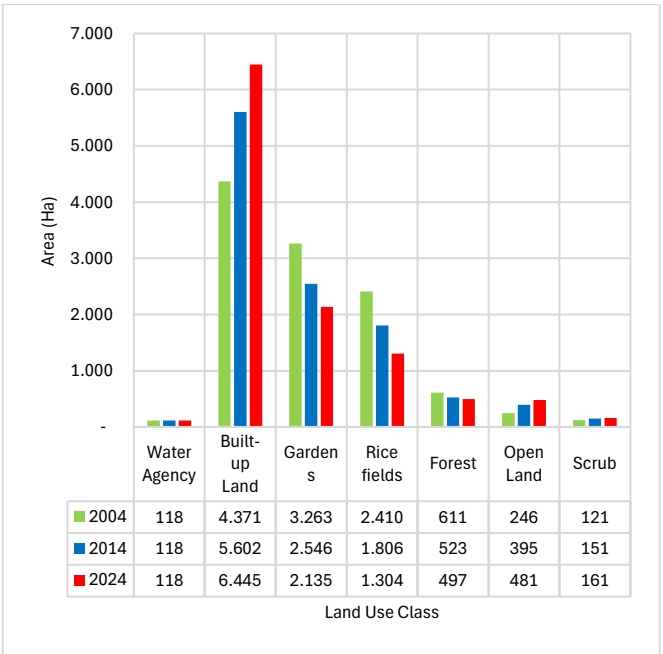


| | Water Agency | Built-up Land | Gardens | Rice fields | Forest | Open Land | Scrub |
|---|---|---|---|---|---|---|---|
| 2004 | 118 | 4.371 | 3.263 | 2.410 | 611 | 246 | 121 |
| 2014 | 118 | 5.602 | 2.546 | 1.806 | 523 | 395 | 151 |
| 2024 | 118 | 6.445 | 2.135 | 1.304 | 497 | 481 | 161 |

**Figure 4.** Graph of Land Use Changes in 2004, 2014, and 2024

Figure 4 shows a graph of changes in land use area in Bogor City in 2004, 2014, and 2024, with a total area of 11,141 ha divided into seven classes. In 2004, developed land covered 4,371 ha (39.2%), gardens covered 3,263 ha (29.3%), rice fields covered 2,410 ha (21.6%), the rest being forest 611 ha, open land 246 ha, water bodies 118 ha, and shrubs 121 ha. In 2014, developed land increased to 5,602 ha (50.3%), while gardens and rice fields decreased to 2,546 ha (22.9%) and 1,806 ha (16.2%). In 2024, built-up land increased sharply to 6,445 ha (57.8%), gardens decreased to 2,135 ha (19.2%), and rice fields to 1,304 ha (11.7%). Open land and scrubland increased slightly. Overall, built-up land dominated, confirming land use change towards urbanization.

### Land Use Accuracy Test

Based on *ground checks*, 117 of 131 field samples were found to be accurate. The samples covered seven land use classes: water bodies, built-up land, gardens, rice fields, forests, open land, and scrubland.

*Producer's Accuracy* for each land use class was

calculated by determining the percentage of correctly classified analysis units with the number of analysis units in that class in the reference data.

$TA = \frac{10}{10} x\ 100\% = 1{,}00 LT = \frac{59}{67} x\ 100\% = 0{,}88$

$, KN = \frac{16}{19} x\ 100\% = 0{,}84 , SH = \frac{8}{8} x\ 100\% = 1{,}00$

$, HN = \frac{8}{9} x\ 100\% = 0{,}89 , LK = \frac{7}{7} x\ 100\% = 1{,}00 ,$

$$SB = \frac{9}{11} x\ 100\% = 1{,}82$$

*User Accuracy* Calculated by calculating the percentage of analysis units that are correctly classified with the number of analysis units in that class in the classification results data.

$TA = \frac{10}{10} x\ 100\% = 1{,}00 , LT = \frac{59}{62} x\ 100\% = 0{,}95 ,$

$KN = \frac{16}{17} x\ 100\% = 0{,}94 , SH = \frac{8}{13} x\ 100\% = 0{,}62 ,$

$HN = \frac{8}{9} x\ 100\% = 0{,}89 , LK = \frac{7}{10} x\ 100\% = 0{,}70 ,$

$$SB = \frac{9}{10} x\ 100\% = 0{,}90$$

*Overall Accuracy* Overall accuracy is calculated by comparing the sample count without *error* to the total sample count. The mathematical calculation is as follows:

$$OA = \frac{10 + 59 + 16 + 8 + 8 + 7 + 9}{131} x\ 100\%$$

$$OA = \frac{117}{131} x\ 100\% = 89.31\%$$

$$Koefisien\ Kappa = \frac{N \sum_{k-1}^{r} X_{kk} - \sum_{k-1}^{r} (X_{k+} \times X_{+k})}{N^2 - \sum_{k-1}^{r} (X_{k+} \times X_{+k})} x\ 100\%$$

$$X_{kk} = (10 + 59 + 16 + 8 + 8 + 7 + 9) = 117$$

$$\sum_{k-1}^{r} (X_{k+} \times X_{+k} = (10x10) + (67x62) + (19x17)$$

$$+ (8x13) + (9x9) + (7x10) + (11x10) = 4.942$$

$$KA = \frac{(117 + 131) - 4.942}{(131^2) - 4.942} x\ 100\% = 84.96\%$$

The analysis results obtained an *Overall Accuracy* value of 89.31%. This study obtained a Kappa coefficient value of 84.96%. This indicates that the Kappa coefficient value is acceptable and quite significant. The classification accuracy values are shown in Table 2.

**Table 2.** Calculation of Land Use Accuracy Test Values

| | | **Field *Ground Check* Results** | | | | | | | | |
|---|---|---|---|---|---|---|---|---|---|---|
| **GEE Classification Results** | Land Use Class | BA | LT | KN | SH | HN | LK | SB | Total Row | *User Accuracy* |
| | BA | 10 | - | - | - | - | - | - | 10 | 1.00 |
| | LT | - | 59 | 2 | - | - | - | 1 | 62 | 0.95 |
| | KN | - | 1 | 16 | - | - | - | - | 17 | 0.94 |
| | SH | - | 3 | 1 | 8 | - | - | 1 | 13 | 0.62 |
| | HN | - | 1 | - | - | 8 | - | - | 9 | 0.89 |
| | LK | - | 2 | - | - | 1 | 7 | - | 10 | 0.70 |
| | SB | - | 1 | - | - | - | - | 9 | 10 | 0.90 |
| | Total Column | 10 | 67 | 19 | 8 | 9 | 7 | 11 | 131 | - |
| | *Producer Accuracy* | 1.00 | 0.88 | 0.84 | 1.00 | 0.89 | 1.00 | 0.82 | - | - |

Description: **BA**: Water Body, **LT**: Built-up Land, **KN**: Garden, **SH**: Rice Field, **HN**: Forest, **LK**: Open Land, **SB**: Shrubbery.
Source: Analysis Results

***Land Surface Temperature***

The results of *Land Surface Temperature* (LST) processing are presented in a thematic map classified based on LST values. This map illustrates the spatial distribution of LST in the city of Bogor. The LST change map is shown in Figure 5, and the graph of LST area changes for the years 2004, 2014, and 2024

of LST in the city of Bogor. The LST change map is

shown in Figure 5 and the graph of LST area change for 2004, 2014, and 2024 is shown in Figure 6.

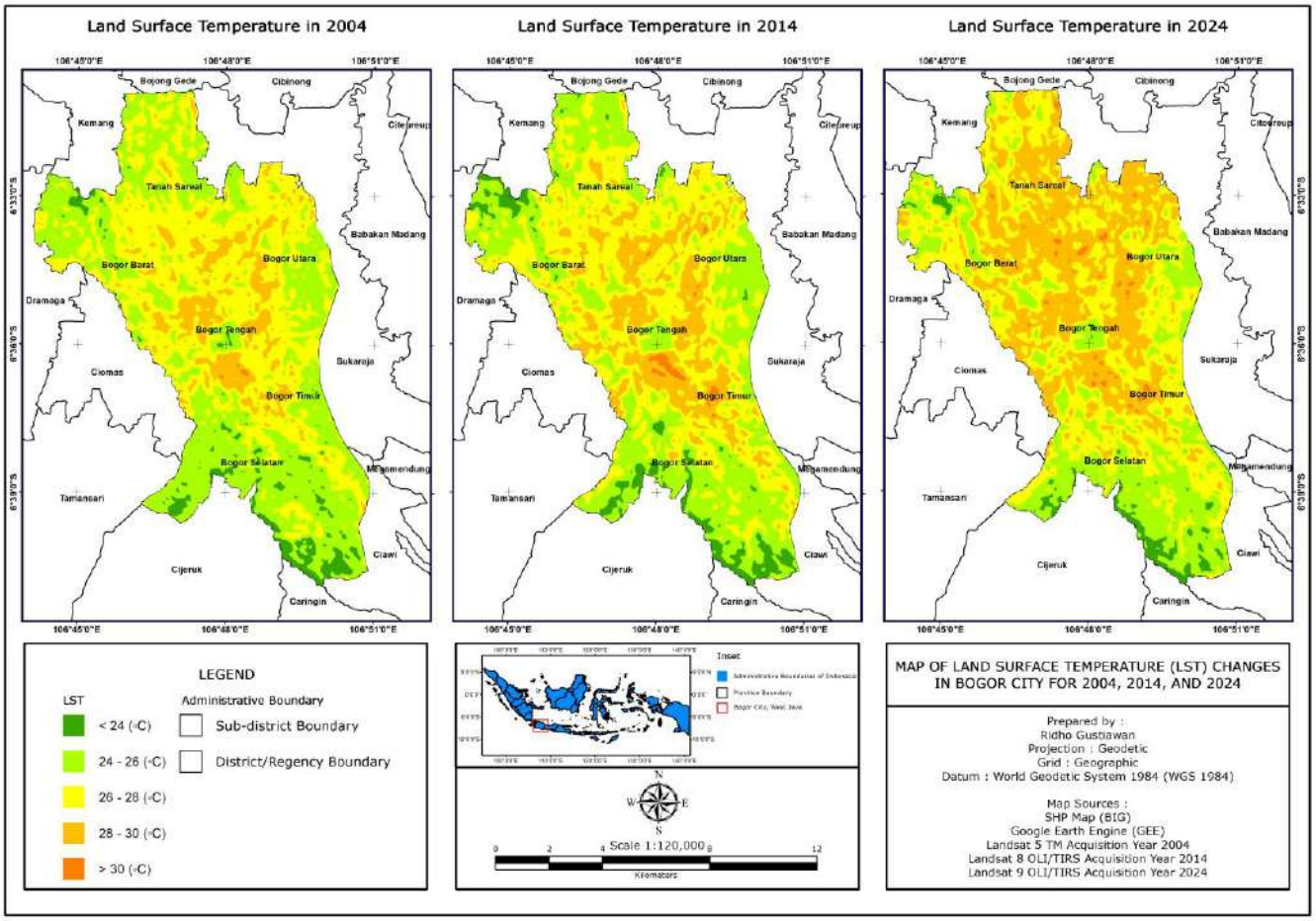


**Figure 5.** Map of *Land Surface Temperature* Changes in 2004, 2014, and 2024

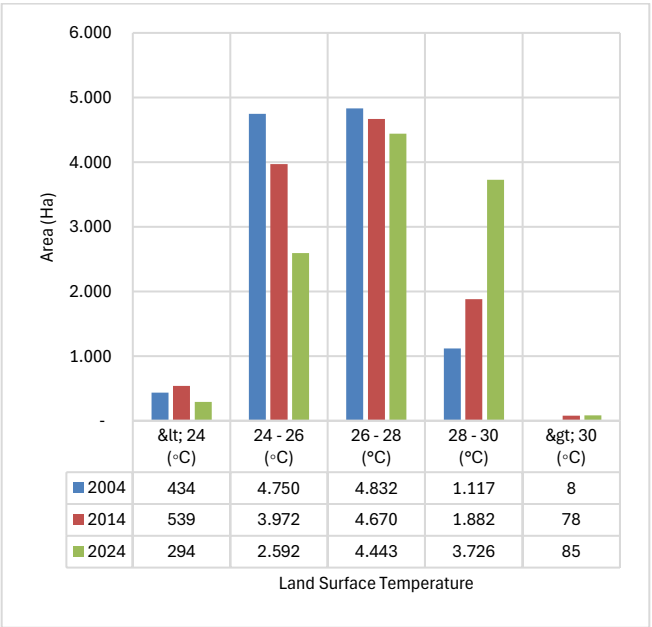


**Figure 6.** Graph of *Land Surface Temperature* Changes in 2004, 2014, and 2024

Figure 6 shows changes in LST distribution in Bogor City in 2004, 2014, and 2024. In 2004, temperatures of 24–26°C dominated 4,750 ha (42.6%), followed by 26–28°C covering 4,832 ha (43.4%). Temperatures of <24°C covered only 434 ha (3.9%) and >28°C covered 1,125 ha (10.1%). In 2014, temperatures <24°C increased to 539 ha (4.8%), while temperatures of 24–26°C decreased to 3,972 ha (35.7%). Temperatures of 26–28°C remained dominant at 4,670 ha (41.9%), and temperatures above 28°C increased to 1,960 ha (17.6%). In 2024, the warming trend was clear: temperatures below 24°C shrank to 294 ha (2.6%), temperatures between 24 and 26°C fell to 2,592 ha (23.3%), temperatures between 26 and 28°C remained widespread (4,443 ha/39.9%), and temperatures above28°C surged to 3,811 ha (34.2%). Overall, LST has increased significantly over the past 20 years, marked by an increase in high-temperature areas and a decrease in low-temperature areas, indicating the impact of global warming or local climate change.

### ***Air Temperature*** **Estimation**

*Air Temperature* ($T_a$) estimates used LST data from Landsat thermal bands and DEM data. A regression model was created with a 500×500 m fishnet grid using the *Create Fishnet* feature in *ArcGIS*. This *grid* extracted the average LST and DEM values for each cell. The regression coefficients of variables $X_{(1)}$(LST) and $X_{(2)}$(DEM) against $T_{(a)}$were calculated to minimize the square error in the training data (AL-Anbari, Jasim, & Mohammed, 2019). The linear regression model follows the equation shown in Table 3.

**Table 3.** *Air Temperature* Estimation Training Data Model

| No | 2004 | | | 2014 | | | 2024 | | |
|---|---|---|---|---|---|---|---|---|---|
| | LST (°C) | DEM | $T_a$(°C) | LST (°C) | DEM | $T_a$ (°C) | LST (°C) | DEM | $T_a$(°C) |
| 1 | 26.45 | 179 | 25.6 | 27.33 | 179 | 28.6 | 27.25 | 179 | 27.5 |
| 2 | 22.60 | 457 | 20.2 | 23.12 | 457 | 22.2 | 24.02 | 457 | 23.6 |
| 3 | 23.89 | 169 | 23.8 | 23.01 | 169 | 24.8 | 23.95 | 169 | 25.5 |
| 4 | 23.68 | 211 | 21.5 | 23.95 | 211 | 22.5 | 24.46 | 211 | 25.6 |
| 5 | 27.51 | 217 | 26.9 | 26.81 | 217 | 27.9 | 27.66 | 217 | 27.6 |
| 6 | 27.72 | 227 | 27 | 27.74 | 227 | 28 | 27.07 | 227 | 27.1 |
| 7 | 28.56 | 240 | 27.6 | 28.54 | 240 | 29.6 | 27.55 | 240 | 27.4 |
| 8 | 24.11 | 293 | 24.1 | 24.38 | 293 | 25.1 | 25.50 | 293 | 24.7 |
| 9 | 22.38 | 414 | 21.4 | 22.36 | 414 | 21.4 | 22.71 | 414 | 21.8 |
| 10 | 26.77 | 157 | 26.2 | 25.77 | 157 | 27.2 | 27.67 | 157 | 27.8 |
| 11 | 25.18 | 179 | 24.2 | 26.66 | 179 | 26.2 | 28.61 | 179 | 28.2 |
| 12 | 26.24 | 184 | 25.9 | 27.43 | 184 | 26.9 | 28.47 | 184 | 28.1 |
| 13 | 20.16 | 365 | 20.7 | 20.16 | 365 | 21.7 | 20.96 | 365 | 23.4 |
| 14 | 26.24 | 218 | 26.1 | 26.94 | 218 | 27.1 | 28.81 | 218 | 28.4 |
| 15 | 24.96 | 195 | 23.8 | 25.77 | 195 | 25.8 | 26.75 | 195 | 28.7 |
| 16 | 22.60 | 421 | 20.8 | 22.54 | 421 | 21.8 | 22.21 | 421 | 20.9 |
| 17 | 24.54 | 366 | 22.7 | 26.75 | 366 | 24.7 | 27.77 | 366 | 27.7 |
| 18 | 26.67 | 237 | 26.5 | 27.25 | 237 | 27.5 | 27.86 | 237 | 26.6 |
| 19 | 28.35 | 253 | 27.2 | 28.33 | 253 | 29.2 | 28.65 | 253 | 28.5 |
| 20 | 29.39 | 255 | 28.7 | 29.72 | 255 | 30.7 | 30.00 | 255 | 30.9 |
| 21 | 25.82 | 298 | 25.3 | 25.04 | 298 | 26.3 | 26.96 | 298 | 25.9 |
| 22 | 28.97 | 275 | 27.3 | 29.32 | 275 | 28.3 | 29.53 | 275 | 28.6 |
| 23 | 25.61 | 157 | 25.5 | 25.50 | 157 | 25.5 | 27.11 | 157 | 27.1 |
| 24 | 26.24 | 167 | 25.9 | 26.01 | 167 | 26.9 | 28.08 | 167 | 28.2 |
| 25 | 25.82 | 170 | 25.6 | 25.97 | 170 | 26.6 | 28.30 | 170 | 28.3 |

Source: Analysis Results & Data from BMKG Stations

The weights of the 2004 linear regression model are:
$y = 2.5702, X_1 = 0.9148, X_2 = -0.0047,$

The weights of the 2014 linear regression model are:
$y = 4.2149, X_1 = 0.9046, X_2 = -0.0060,$

The weights of the 2024 linear regression model are:
$y = 8.0120, X_{(1)} = 0.7614, X_{(2)} = -0.0065.$

The estimation results are presented in a thematic map showing the spatial distribution *of air temperature* in Bogor City. The change map and area graph (Ha) for 2004, 2014, and 2024 were calculated using the *Calculate Geometry* feature in *ArcGIS* and are shown in Figures 7 and 8.

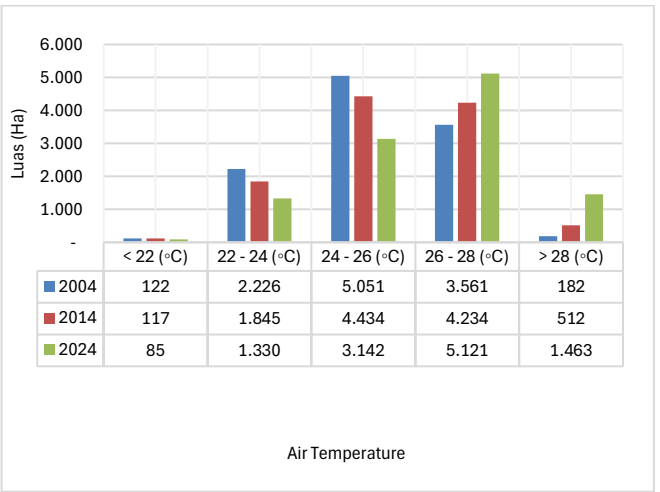


**Figure 8.** *Air Temperature* Change Graph for 2004, 2014, and 2024

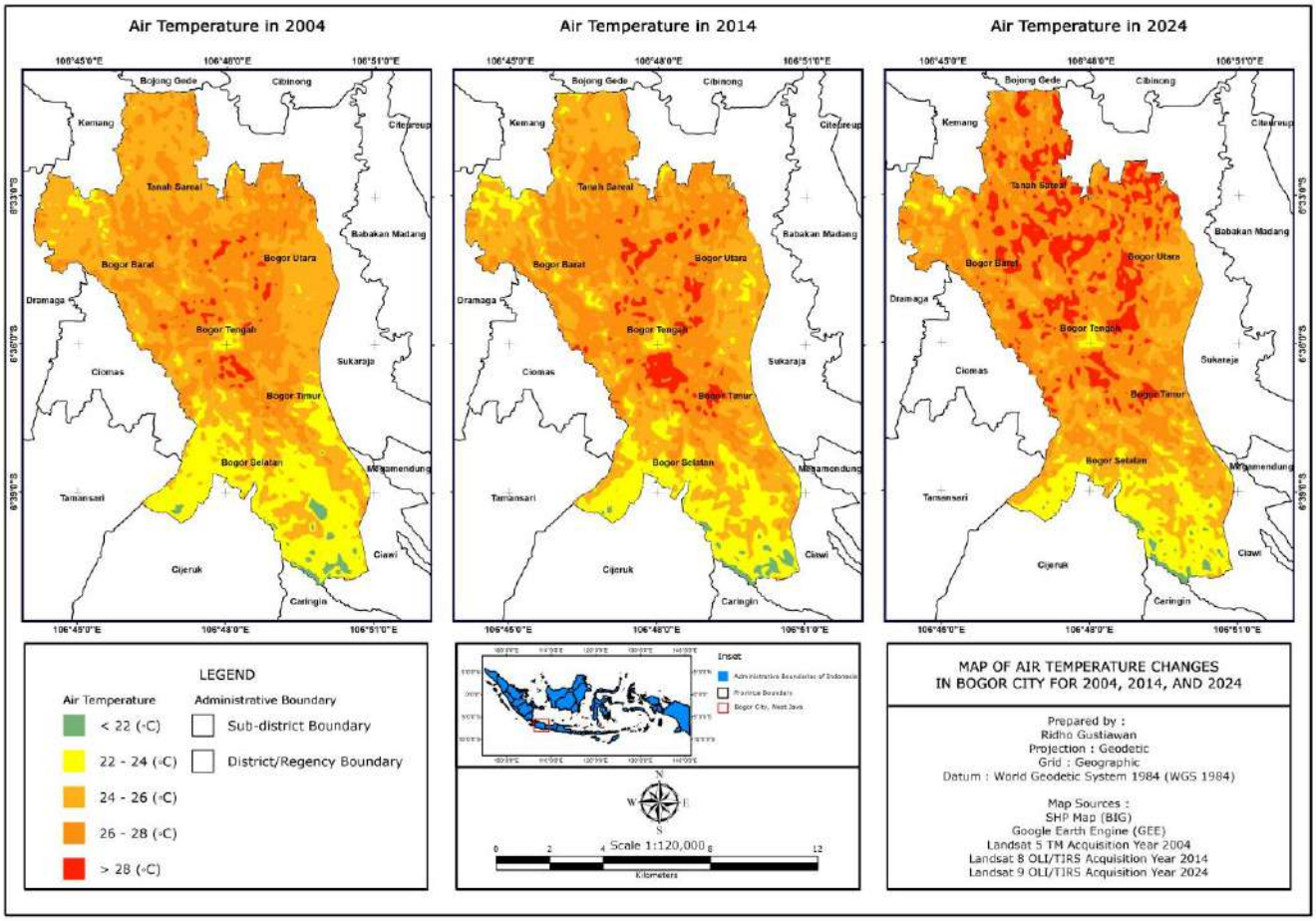


**Figure 7.** *Air Temperature* Change Map for 2004, 2014, and 2024

Figure 8 shows changes in air temperature (Ta) distribution in Bogor City in 2004, 2014, and 2024. In 2004, temperatures of 24–26°C dominated 5,051 ha (45.34%), followed by 26–28°C covering 3,561 ha (31.96%). Temperatures of <22°C covered only 122 ha (1.09%), 22–24°C covered 2,226 ha (19.98%), and >28°C covered 181 ha (1.63%). In 2014, temperatures <22°C decreased to 117 ha (1.05%), 22–24°C to 1,845 ha (16.56%), and 24–26°C to 4,434 ha (39.80%), while 26–28°C increased to 4,234 ha (38.02%) and >28°C to 511 ha (4.59%). In 2024, <22°C decreased to 85 ha (0.76%), 22–24°C decreased to 1,330 ha (11.94%), 24–26°C decreased to 3,142 ha (28.22%), while 26–28°C increased to 5,112 ha (45.97%) and >28°C jumped to 1,463 ha (13.13%). Overall, there was an upward trend in air temperature, marked by the expansion of high-temperature areas (26–28°C and >28°C) and a reduction in low-temperature areas (<26°C), indicating local warming in the city of Bogor.

The validation was carried out by comparing the air temperature predicted by the linear regression model with BMKG data (annual average) for 2004, 2014, and 2024. Figure 9 shows a graph comparing the prediction results with BMKG data to assess the accuracy of the model.

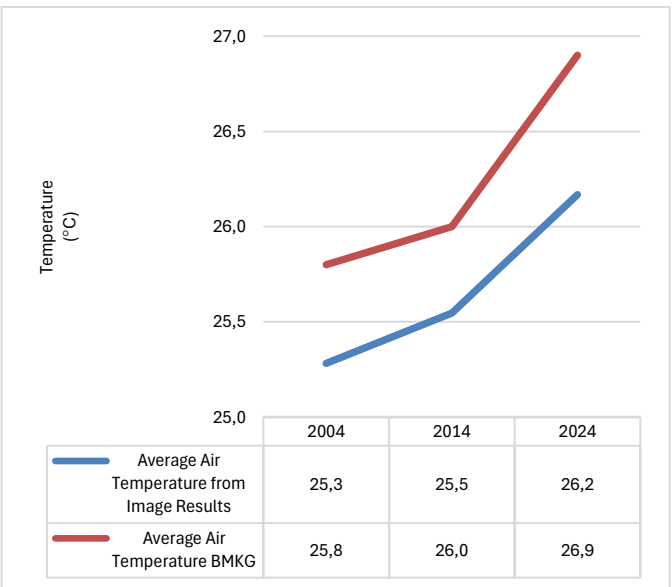


**Figure 10.** Average *Air Temperature* Comparison Graph

Figure 10 shows that the average air temperature in Bogor City rose from 25.3°C (2004) to 26.2°C (2024) based on imagery, while BMKG data rose from 25.8°C to 26.9°C. The trends are consistent, but there is a difference due to the different methods used: BMKG uses monthly averages from 24-hour daily measurements, while the imagery records instantaneous temperatures when the Landsat satellite passes overhead. The difference in acquisition time affects the values, but does not change the upward trend.

***Relative Humidity* Estimation**

*Relative Humidity* (RH) estimates use LST and NDVI data from processed Landsat images. NDVI is calculated from the NIR and Red bands according to sensor specifications. The regression coefficients for variables $X_1$ (LST) and $X_2$ (NDVI) against RH are obtained through a linear regression model according to the equation in Table 4.

**Table 4.** *Relative Humidity* Estimation Training Data Model

| No | 2004 | | | 2014 | | | 2024 | | |
|---|---|---|---|---|---|---|---|---|---|
| | LST (°C) | NDVI | RH (%) | LST (°C) | NDVI | RH (%) | LST (°C) | NDVI | RH (%) |
| 1 | 26.45 | 0.32 | 86 | 27.33 | 0.20 | 84 | 27.25 | 0.17 | 85 |
| 2 | 22.60 | 0.23 | 88 | 23.12 | 0.18 | 90 | 24.02 | 0.22 | 92 |
| 3 | 23.89 | 0.26 | 85 | 23.01 | 0.13 | 87 | 23.95 | 0.02 | 79 |
| 4 | 23.68 | 0.33 | 87 | 23.95 | 0.28 | 89 | 24.46 | 0.18 | 87 |
| 5 | 27.51 | 0.36 | 84 | 26.81 | 0.10 | 86 | 27.66 | 0.07 | 82 |
| 6 | 27.72 | 0.26 | 82 | 27.74 | 0.11 | 84 | 27.07 | 0.09 | 83 |
| 7 | 28.56 | 0.25 | 81 | 28.54 | 0.11 | 80 | 27.55 | 0.12 | 84 |
| 8 | 24.11 | 0.28 | 88 | 24.38 | 0.11 | 88 | 25.50 | 0.09 | 88 |
| 9 | 22.38 | 0.26 | 90 | 22.36 | 0.18 | 94 | 22.71 | 0.19 | 91 |
| 10 | 26.77 | 0.21 | 80 | 25.77 | 0.24 | 86 | 27.67 | 0.15 | 81 |
| 11 | 25.18 | 0.36 | 86 | 26.66 | 0.25 | 85 | 28.61 | 0.19 | 78 |
| 12 | 26.24 | 0.27 | 83 | 27.43 | 0.22 | 84 | 28.47 | 0.14 | 77 |
| 13 | 20.16 | 0.21 | 90 | 20.16 | 0.16 | 96 | 20.96 | 0.15 | 94 |
| 14 | 26.24 | 0.38 | 84 | 26.94 | 0.14 | 82 | 28.81 | 0.15 | 76 |
| 15 | 24.96 | 0.31 | 83 | 25.77 | 0.30 | 90 | 26.75 | 0.26 | 89 |
| 16 | 22.60 | 0.29 | 88 | 22.54 | 0.23 | 95 | 22.21 | 0.18 | 92 |
| 17 | 24.54 | 0.28 | 85 | 26.75 | 0.15 | 87 | 27.77 | 0.12 | 83 |
| 18 | 26.67 | 0.28 | 84 | 27.25 | 0.27 | 88 | 27.86 | 0.21 | 84 |
| 19 | 28.35 | 0.25 | 80 | 28.33 | 0.09 | 78 | 28.65 | 0.08 | 78 |
| 20 | 29.39 | 0.27 | 78 | 29.72 | 0.10 | 76 | 30.00 | 0.10 | 70 |
| 21 | 25.82 | 0.41 | 88 | 25.04 | 0.23 | 87 | 26.96 | 0.29 | 91 |
| 22 | 28.97 | 0.22 | 77 | 29.32 | 0.15 | 78 | 29.53 | 0.17 | 75 |
| 23 | 25.61 | 0.26 | 85 | 25.50 | 0.21 | 85 | 27.11 | 0.16 | 81 |
| 24 | 26.24 | 0.31 | 86 | 26.01 | 0.19 | 84 | 28.08 | 0.16 | 79 |
| 25 | 25.82 | 0.32 | 87 | 25.97 | 0.23 | 86 | 28.30 | 0.18 | 80 |

Source: Analysis Results & Data from BMKG Station

The linear regression model weights for 2004 are: Y = 112.4678, $X_1$ = -1.3479, $X_2$ = 23.1878, The linear regression model weights for 2014 are: Y = 128.6706, $X_1$ = -1.7825, $X_2$ = 18.548, The linear regression model weights for 2024 are: Y = 131.3131, $X_1$ = -2.0303, $X_2$ = 39.7353.

*The Relative Humidity* (RH) estimation results are presented in a thematic map classified based on RH values. This map shows the spatial distribution of RH in Bogor City, as shown in Figure 11, while the graph of changes in RH area (hectares) for 2004, 2014, and 2024 is shown in Figure 12.

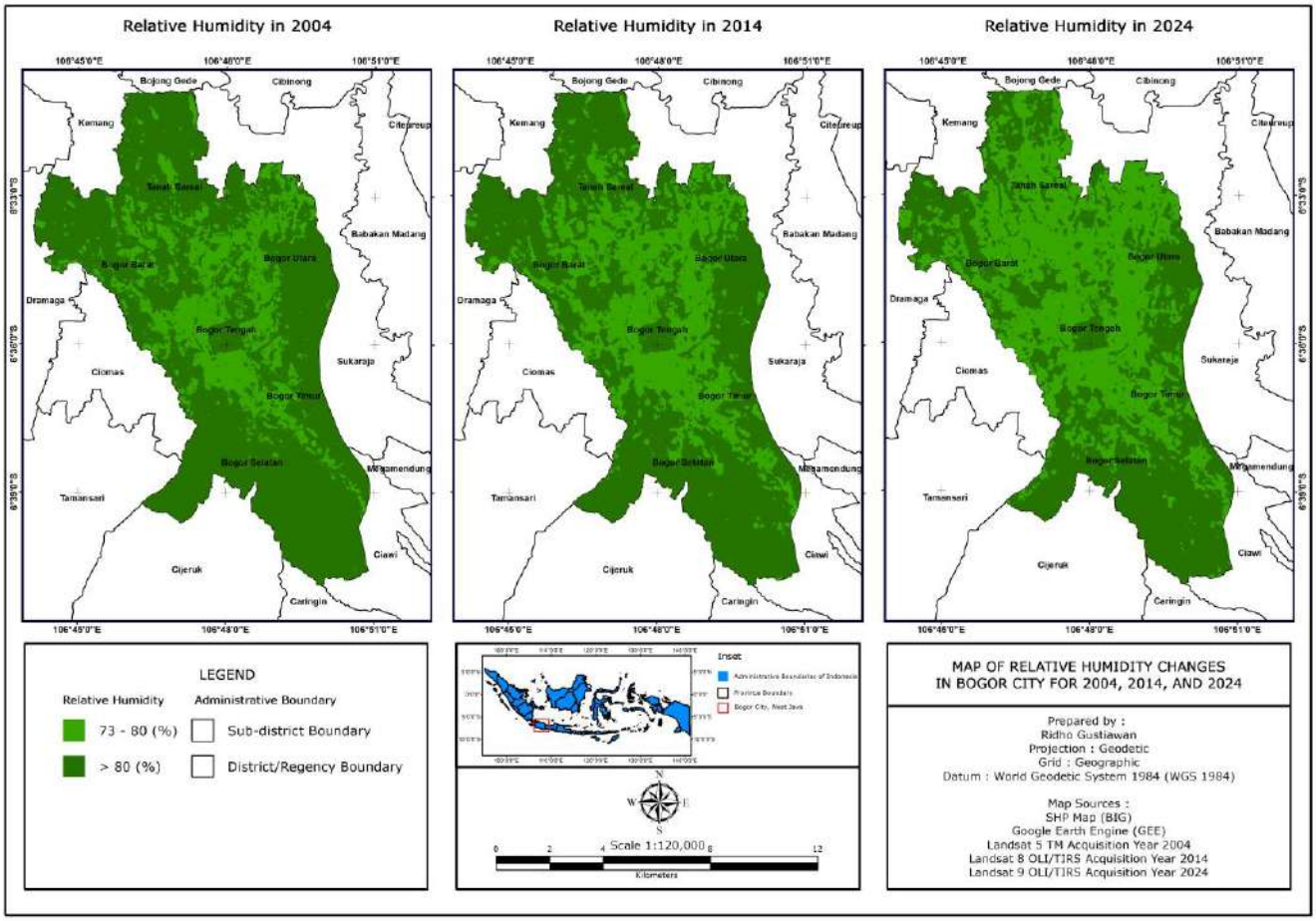


**Figure 11.** Map of *Relative Humidity* Changes in 2004, 2014, and 2024

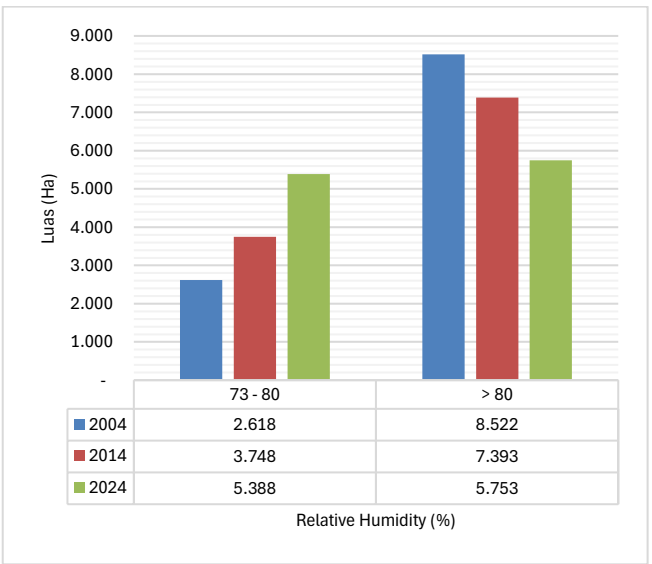


| | 73 - 80 | > 80 |
|---|---|---|
| 2004 | 2.618 | 8.522 |
| 2014 | 3.748 | 7.393 |
| 2024 | 5.388 | 5.753 |

**Figure 12.** Graph of *Relative Humidity* Changes in 2004, 2014, and 2024

Figure 12 shows changes in RH distribution in Bogor City in 2004, 2014, and 2024. In 2004, high humidity (>80%) dominated 8,522 ha (76.5%), while moderate humidity (74–80%) dominated 2,618 ha (23.5%). In 2014, moderate humidity increased to 3,748 ha (33.6%), while high humidity decreased to 7,393 ha (66.4%). In 2024, moderate humidity increased significantly to 5,388 ha (48.4%), while high humidity decreased to 5,753 ha (51.6%). Overall, there has been a shift from high to moderate humidity in the last 20 years.

Validation was carried out using RH data from the BMKG Climate Station in Bogor City. The results are shown in Figure 12.

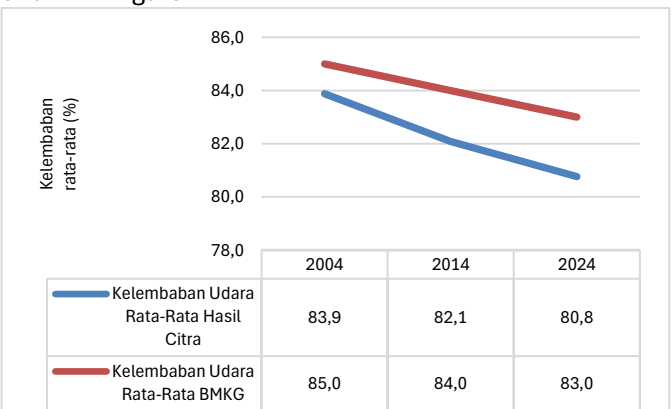


| | 2004 | 2014 | 2024 |
|---|---|---|---|
| Kelembaban Udara Rata-Rata Hasil Citra | 83,9 | 82,1 | 80,8 |
| Kelembaban Udara Rata-Rata BMKG | 85,0 | 84,0 | 83,0 |

**Figure 13.** Average *Relative Humidity* Comparison Graph

The results of the study show that the average RH from satellite imagery decreased from 83.9% (2004) to 80.8% (2024). A similar trend was seen in BMKG data, which decreased from 85.0% to 83.0% over the same period.

**Temperature Humidity Index**

The results of the Temperature Humidity Index (THI) processing are presented in the form of thematic maps classified based on THI values. These maps show the spatial distribution of THI in Bogor City for 2004, 2014, and 2024, as shown in Figure 14. In addition, graphs showing changes in area based on THI values in hectares for 2004, 2014, and 2024 are also presented. This data was calculated using the Calculate Geometry feature in ArcGIS and is shown in Figure 15.

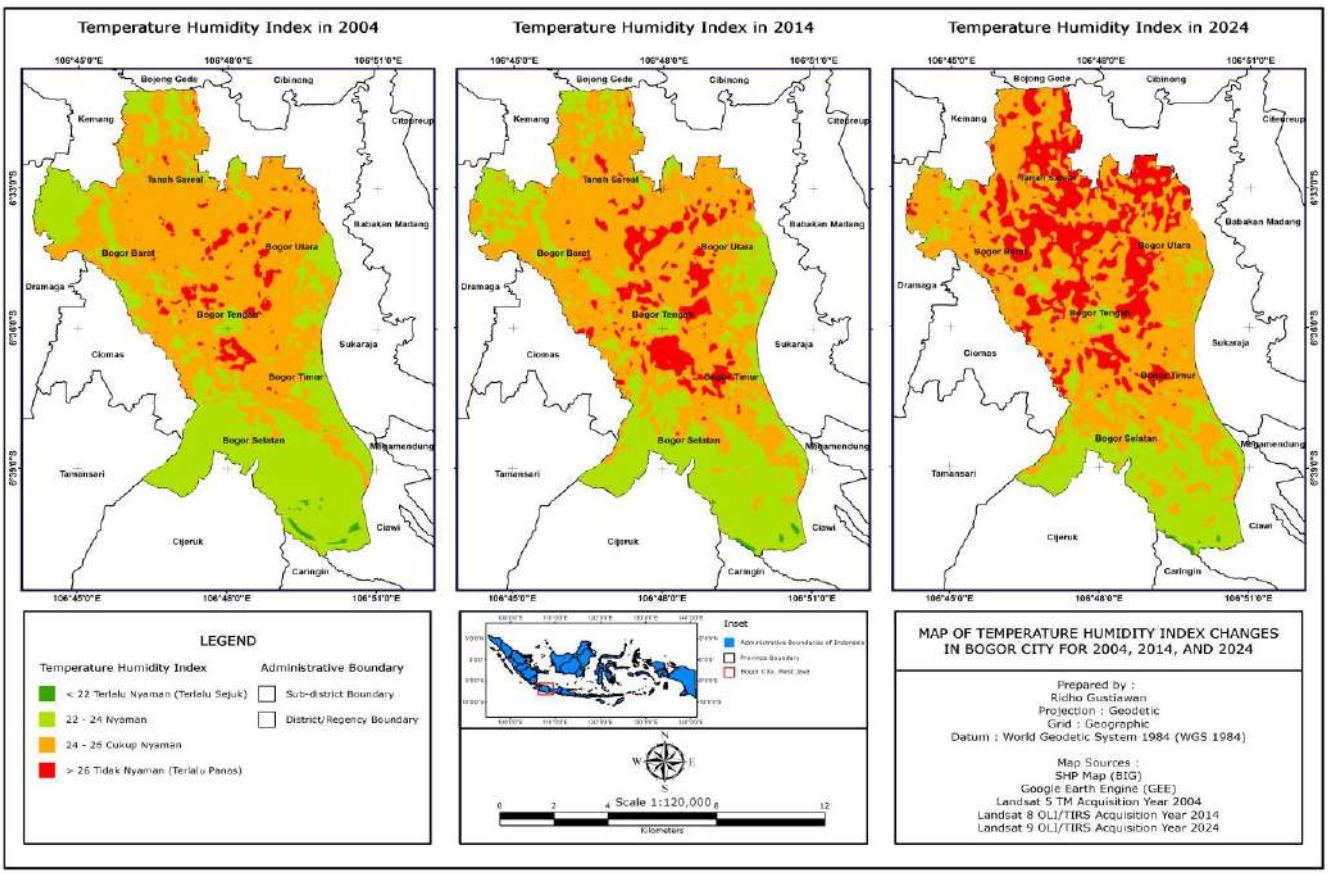


**Figure 15.** Map of *Temperature Humidity Index* Changes in 2004, 2014, and 2024

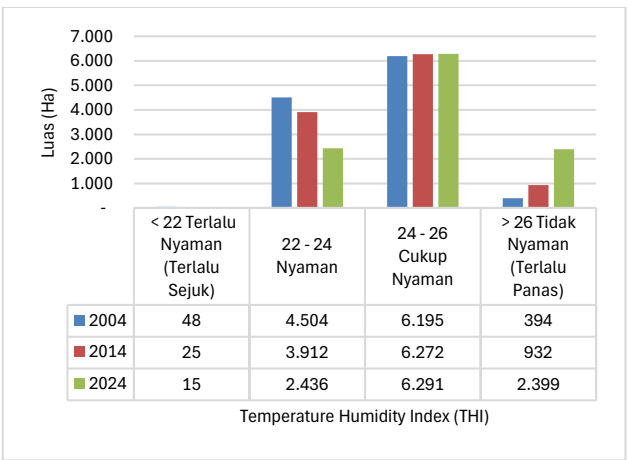


| | < 22 Terlalu Nyaman (Terlalu Sejuk) | 22 - 24 Nyaman | 24 - 26 Cukup Nyaman | > 26 Tidak Nyaman (Terlalu Panas) |
|---|---|---|---|---|
| 2004 | 48 | 4.504 | 6.195 | 394 |
| 2014 | 25 | 3.912 | 6.272 | 932 |
| 2024 | 15 | 2.436 | 6.291 | 2.399 |

**Figure 16.** Graph of *Temperature Humidity Index* Changes in 2004, 2014, and 2024

Figure 16 shows changes in THI distribution in Bogor City in 2004, 2014, and 2024. In 2004, THI <22 (too cool) was 48 ha (0.43%), THI 22–24 (comfortable) dominated 4,504 ha (40.42%), THI 24–26 (quite comfortable) 6,195 ha (55.61%), and THI >26 (too hot) 394 ha (3.54%). In 2014, the area that was too cool decreased to 25 ha (0.23%), the comfortable area became 3,912 ha (35.11%), the fairly comfortable area increased slightly to 6,272 ha (56.30%), and the too hot area increased to 932 ha (8.36%). In 2024, conditions worsened: the area that was too cool remained at 15 ha (0.14%), the comfortable area decreased to 2,436 ha (21.86%), the fairly comfortable area remained stable at 6,291 ha (56.47%), but the area that was too hot jumped to 2,399 ha (21.53%). Overall, there was a decrease in

comfortable areas and a significant increase in excessively hot areas throughout 2004–2024.

**Analysis of the Relationship Between Land Use and *Land Surface Temperature* and *Temperature Humidity Index***

Changes in land use, which were dominated by an increase in built-up land, were analyzed in relation to the variables LST, NDVI, air temperature, RH, and THI. The analysis used grouping graphs to see the trend of the relationship between land changes and each variable, both increasing and decreasing. The relationship patterns between variables are shown in Figures 17–21.

The graph of the relationship between built-up land and NDVI shows a decrease in NDVI values from 0.288 (2004) to 0.227 (2014) and 0.210 (2024), indicating a reduction in vegetation cover.

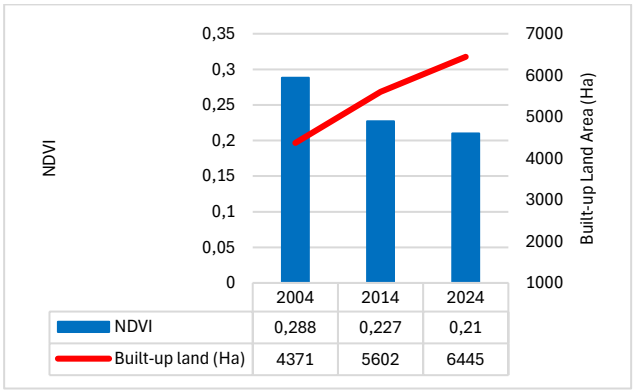


**Figure 17.** Trend Graph of the Relationship Between Built-Up Land and NDVI

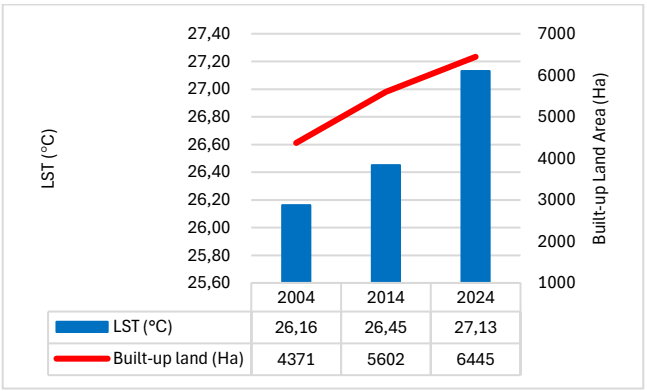


**Figure 18.** Trend Graph of Changes in the Relationship Between Developed Land and LST

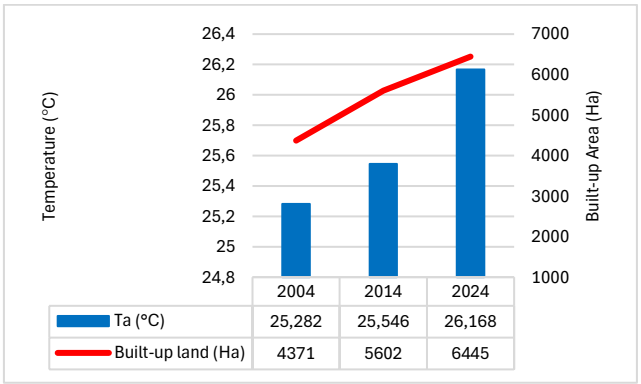


**Figure 19.** Trend Graph of Changes in the Relationship Between Built-Up Land and Air Temperature

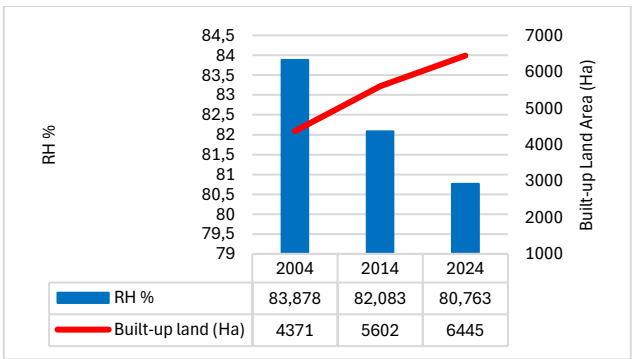


**Figure 20.** Trend Graph of Changes in the Relationship Between Built-Up Land and RH

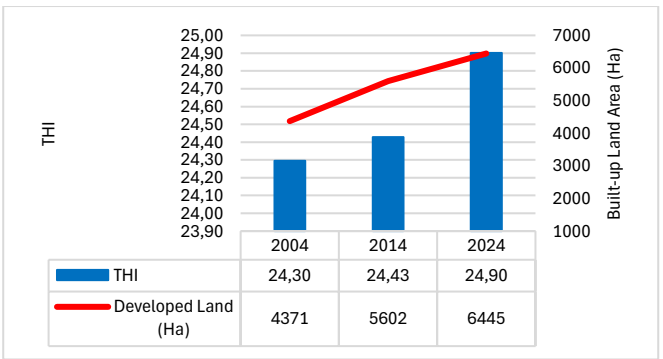


**Figure 21.** Trend Graph of the Relationship Between Built-up Land and THI

The graph of the relationship with LST shows an increase in surface temperature from 26.16°C to 27.13°C, while the Ta graph shows an increase in air temperature from 25.28°C to 26.17°C. The RH graph shows a decrease in humidity from 80.88% (2004) to 80.76% (2024), indicating that the air is getting drier. The THI graph shows an increase from 24.30 to 24.90, indicating a rise in discomfort levels. Overall, the five graphs illustrate that the increase in built-up land in Bogor City during 2004–2024 correlates with rising temperatures, declining vegetation, and decreasing humidity.

**Web Application Development**

A web application based on *Google Earth Engine Apps* has been successfully developed to display analysis results in an interactive and *user-friendly* manner. This application provides *real-time* information on land use changes, LST, air temperature, RH, and THI. The application can be accessed via the link: https://ee-rdhgstwnn18.projects.earthengine.app/view/perubahan-land-use-lst-dan-thi-kota-bogor-2014-2014-2024, as shown in Figure 22.

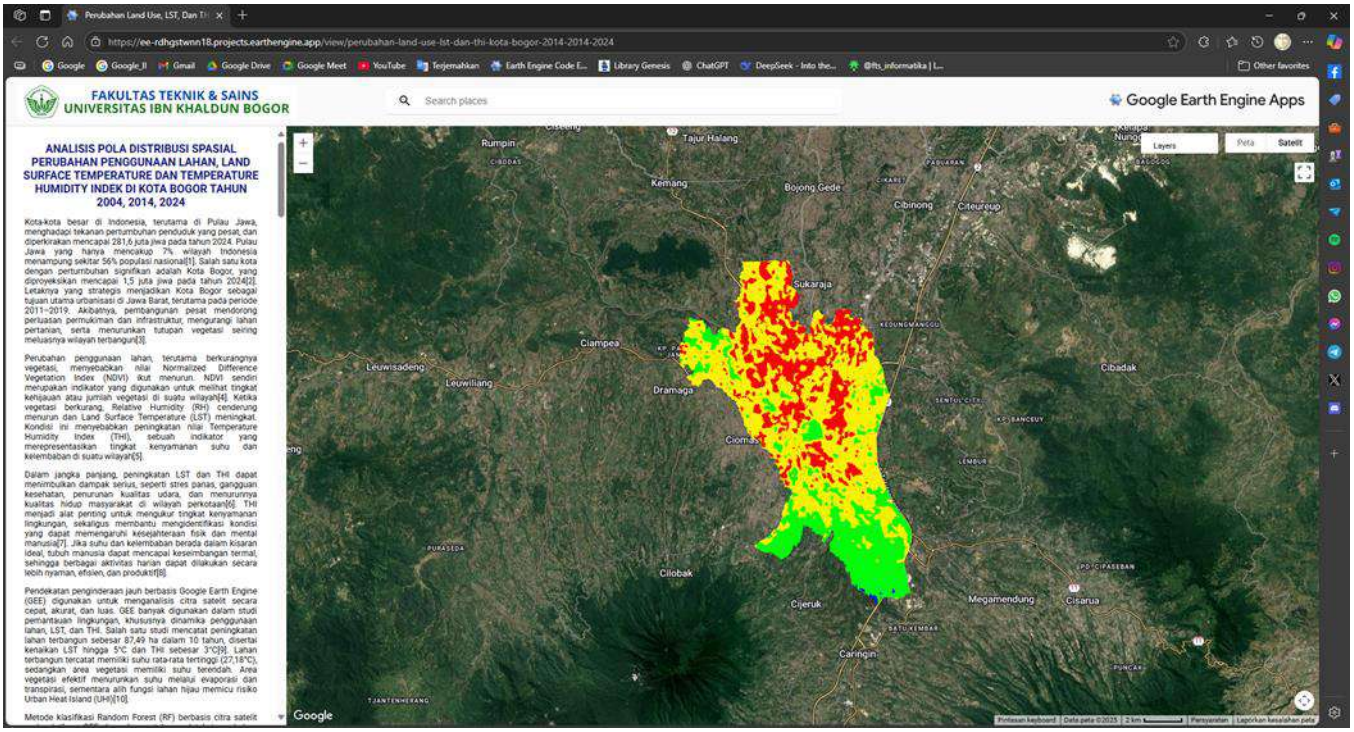


**Figure 22.** *Google Earth Engine Apps* Web Application Page

## CONCLUSION

Based on the results of spatial analysis of land use change, *Land Surface Temperature* (LST), and *Temperature Humidity Index* (THI) in Bogor City in 2004, 2014, and 2024, several conclusions can be drawn to answer the research questions. The following are some of the conclusions:

Land use transformation in Bogor City during the period 2004 to 2024 shows significant changes, marked by an increase in built-up land area from 4,371 hectares (39.2%) in 2004 to 6,445 hectares (57.8%) in 2024. This conversion mainly replaced vegetation areas such as gardens, rice fields, and forests. As a result, there was an increase in the area with high LST (28–30 °C) from 1,117 hectares to 3,726 hectares, as well as an increase in the area with "too hot" THI (THI > 26) from 394 hectares to 2,399 hectares. Meanwhile, the area with a "comfortable" THI (THI 22–24) decreased dramatically from 4,504 hectares to 2,436 hectares. This fact indicates that urbanization has caused a significant degradation of environmental comfort.

There is a strong correlation between the increase in built-up land and the increase in LST and THI. The increase in built-up land area from 4,371 hectares (2004) to 6,445 hectares (2024) contributed directly to the increase in average LST from 26.16 °C to 27.13 °C and the increase in THI from 24.30 to 24.90. These results show that the conversion of vegetation to settlements accelerates the phenomenon of local warming and worsens thermal comfort in urban areas.

*A Google Earth Engine Apps*-based web application was successfully developed as an interactive visualization tool. This application presents spatial and temporal changes in land use, LST, and THI in 2004, 2014, and 2024 in a dynamic and easily accessible manner. This platform has proven effective in visually communicating the results of the analysis to policymakers and the public, supporting spatial data-based urban planning.

Although this study successfully provides an overview of the relationship between land use change and thermal conditions, there are several limitations that need to be considered. LST and THI estimates based on Landsat images with a resolution of 30 meters mean that details in narrow areas such as small roads or urban green spaces are not optimally recorded. In addition, THI calculations using a simple formula only consider air temperature and relative humidity, without including other climatic factors such as wind speed and solar radiation, which also affect thermal comfort.

For further research, it is recommended to include additional climate variables such as rainfall, solar radiation, and wind speed and direction to provide a more comprehensive picture of urban climate conditions. The use of satellite imagery with higher spatial resolution, such as Sentinel-2A, is also recommended to improve the accuracy of mapping and calculation of environmental parameters. Imagery with better resolution can improve accuracy in mapping and calculation of environmental parameters, including LST and THI.

**Acknowledgements** We would like to thank Ibn Khaldun University Bogor for providing academic support in conducting this research. We would also like to express our appreciation to the Meteorology, Climatology, and Geophysics Agency (BMKG) and *the United States Geological Survey* (USGS) for providing supporting data in the form of climate data and Landsat satellite images. Thanks are also extended to the Supervising Lecturer and Examination Team for their guidance, mentoring, and valuable input during the research and writing process. This research was funded by the Author's Independent Funds without external grant support.

**Conflict of Interest** The author has no competing interests to declare that are relevant to the content of this article.



## REFERENCES

AL-Anbari, R. H., Jasim, O. Z., & Mohammed, Z. T. (2019). Estimation High Resolution Air Temperature Based on landsat8 images and Climate Datasets. *IOP Conference Series: Materials Science and Engineering*, *518*(2), 22–33. Institute of Physics Publishing. Retrieved from https://iopscience.iop.org/article/10.1088/1757-899X/518/2/022033

Azahra, S. D., & Kartikawati, S. M. (2021). Tingkat Kenyamanan Termal Ruang Terbuka Hijau dengan Pendekatan Temperature Humidity Index (THI). *BIOEDUSAINS:Jurnal Pendidikan Biologi dan Sains*, *4*(1), 40–47. IPM2KPE. Retrieved from https://journal.ipm2kpe.or.id/index.php/BIOEDUSAINS/article/view/2286

Badan Pusat Statistik (BPS). (2025, May 2). Penduduk, Laju Pertumbuhan Penduduk, Distribusi Persentase Penduduk, Kepadatan Penduduk, Rasio Jenis Kelamin Penduduk Menurut Provinsi, 2024. *BPS*. Retrieved May 11, 2025, from https://www.bps.go.id/id/statistics-table/3/V1ZSbFRUY3lTbFpEYTNsVWNGcDZjek53YkhsNFFUMDkjMyMwMDAw/jumlah-penduduk--laju-pertumbuhan-penduduk--distribusi-persentase-penduduk--kepadatan-penduduk--rasio-jenis-kelamin-penduduk-menurut-provinsi.html?year=2024

Baihaqi, H. F., Prasetyo, Y., & Bashit, N. (2020). Analisis Perkembangan Kawasan Industri Kendal Terhadap Perubahan Suhu Permukaan (Studi Kasus: Kawasan Industri Kendal, Kabupaten Kendal). *Jurnal Geodesi UNDIP*, *9*, 176–186. Retrieved July 25, 2025, from https://doi.org/10.14710/jgundip.2020.26162

Cardille, J. A., Crowley, M. A., Saah, D., & Clinton, N. E. (2024). *Cloud-Based Remote Sensing with Google Earth Engine*. (J. A. Cardille, M. A. Crowley, D. Saah, & N. E. Clinton, Eds.)*Cloud-Based Remote Sensing with Google Earth Engine: Fundamentals and Applications*. Cham: Springer International Publishing. Retrieved from https://link.springer.com/10.1007/978-3-031-26588-4

Congalton, R. G., & Green, K. (2008). *Assessing the Accuracy of Remotely Sensed Data*. Boca Raton,

London, New York: CRC Press. Retrieved from https://www.taylorfrancis.com/books/9781420055139

Damayanti, R., Safe'i, R., Setiawan, A., & Yuwono, S. B. (2023). Analisis Tingkat Kenyamanan Berdasarkan Temperature Humidity Index (THI) Di Hutan Kota Terminal 16C, Hutan Kota Tesarigaga dan Hutan Kota Islamic Center Kota Metro Lampung. *Jurnal Hutan Tropis*, *11*(3), 364. Cetak. Retrieved from https://ppjp.ulm.ac.id/journal/index.php/jht/article/view/17631

Ebi, K. L., Burton, I., & McGregor, G. R. (2009). *Biometeorology for Adaptation to Climate Variability and Change*. (K. L. Ebi, I. Burton, & G. R. McGregor, Eds.). Dordrecht: Springer Netherlands. Retrieved from http://link.springer.com/10.1007/978-1-4020-8921-3

Effendy, S. (2007). *Keterkaitan Ruang Terbuka Hijau dengan Urban Heat Island Wilayah JABOTABEK*. Sekolah Pascasarjana, Institut Pertanian Bogor, Bogor.

Erkamim, M., Mukhlis, I. R., Putra, Adiwarman, M., Rassarandi, F. D., Rumata, N. A., Arrofiqoh, E. N., et al. (2023). *Sistem Informasi Geografis (SIG) Teori Komprehensif SIG*. Bantul, Daerah Istimewa Yogyakarta: PT. Green Pustaka Indonesia.

Fauzi, F., Kharisudin, I., Wasono, R., Utami, T. W., & Harmoko, I. W. (2023). Thermal Stress Projection Based On Temperature-Humidity Index (THI) Under Climate Change Scenario. *Jurnal Meteorologi dan Geofisika*, *24*(1), 65–73. Retrieved from https://jmg.bmkg.go.id/jmg/index.php/jmg/article/view/867

Hansen, J., Ruedy, R., Sato, M., & Lo, K. (2010). GLOBAL SURFACE TEMPERATURE CHANGE. *Reviews of Geophysics*, *48*(4), RG4004. Blackwell Publishing Ltd. Retrieved July 25, 2025, from http://doi.wiley.com/10.1029/2010RG000345

Hardjo, K. S., & Susila, E. T. (2025). A Comparative Analysis of RG-NIR and Multispectral Camera Imagery Acquired via Unmanned Aerial Vehicles for Sugarcane Crop Detection, *13*(1), 113–126. Retrieved July 25, 2025, from http://dx.doi.org/10.23960/jpg

Insan, A. F. N., & Prasetya, F. V. A. S. (2021). Sebaran Land Surface Temperature Dan Indeks Vegetasi Di Wilayah Kota Semarang Pada Bulan Oktober 2019. *Buletin Poltanesa*, *22*(1). Politeknik Pertanian Negeri Samarinda. Retrieved from http://e-journal.politanisamarinda.ac.id/index.php/tanesa/article/view/471

Ita Selvia, S., Virgota, A., Arifin Aria Bakti, L., Sukartono, & Hari Kusumo, B. (2025). Drought in West Sumbawa: Non-Structural Mitigation Efforts Through Mapping and Policy Recommendations, *13*(1), 99–112. Retrieved July 25, 2025, from http://dx.doi.org/10.23960/jpg

Jing, S., Li, B., Tan, M., & Liu, H. (2013). Impact of Relative Humidity on Thermal Comfort in a Warm Environment. *Indoor and Built Environment*, *22*(4), 598–607. Retrieved July 25, 2025, from https://doi.org/10.1177/1420326X12447614

M, A., Ahmed, S. A., & N, H. (2023). Land use and land cover classification using machine learning algorithms in google earth engine. *Earth Science Informatics*, *16*(4), 3057–3073. Retrieved from https://doi.org/10.1007/s12145-023-01073-w

Noviani, R., Saputra, A. E., Wijayanti, P., & Koesoma, S. (2024). Analysis of Land Use Land Cover and Land Surface Temperature in Karst Area: A Case Study Wonogiri Regency. *Indonesian Journal Of Applied Physics*, *14*(1), 89. UNS Solo. Retrieved from https://jurnal.uns.ac.id/ijap/article/view/79048

Nugroho, A. S., Wijaya, P. A., & Sukmono, A. (2016). Analisis Pengaruh Perubahan Vegetasi terhadap Suhu Permukaan di Wilayah Kabupaten Semarang Menggunakan Metode Penginderaan Jauh. *Jurnal Geodesi Undip*, *5(1)*, 253–263.

Prasad, V. K., Ray, S. S., & Justice, C. (2022). *Remote Sensing of Agriculture and Land Cover/Land Use Changes in South and Southeast Asian Countries*. (K. P. Vadrevu, T. Le Toan, S. S. Ray, & C. Justice, Eds.). Cham: Springer International Publishing. Retrieved from https://link.springer.com/10.1007/978-3-030-92365-5

Raharjo, B. (2022). *Deep Learning dengan Python*. Semarang: Yayasan Prima Agus Teknik (YPAT).

Reja, P. D., Riyadi, R., & Mujiati, M. (2020). Kesesuaian Perubahan Penggunaan Tanah Tahun 2011-2019 Terhadap RTRW Di Kota Bogor. *Tunas Agraria*, *3*(3). Retrieved from https://jurnaltunasagraria.stpn.ac.id/index.php/JT

A/article/view/128

Samsu Rijal, S. (2020). *Mengolah Citra Pengindraan Jauh dengan Google Earth Engine*. Yogyakarta: Deepublish Publisher (Grup Penerbitan CV Budi Utama).

Sheykhmousa, M., Mahdianpari, M., Ghanbari, H., Mohammadimanesh, F., Ghamisi, P., & Homayouni, S. (2020). Support Vector Machine Versus Random Forest for Remote Sensing Image Classification: A Meta-Analysis and Systematic Review. *IEEE Journal of Selected Topics in Applied Earth Observations and Remote Sensing*, *13*, 6308–6325. Institute of Electrical and Electronics Engineers Inc. Retrieved from https://ieeexplore.ieee.org/document/9206124/

Spiridonov, V., & Ćurić, M. (2021). Air Temperature. In V. Spiridonov & M. Ćurić (Eds.), *Fundamentals of Meteorology* (pp. 73–86). Cham: Springer International Publishing. Retrieved from http://link.springer.com/10.1007/978-3-030-52655-9_7

Susetyo, B. (2010). *Statistika untuk Analisis Data Penelitian: Dilengkapi Cara Perhitungan dengan SPSS dan MS Office Excel*. Bandung: PT Refika Aditama.

Winarno, D. G., Harianto, P. S., & Santoso, R. (2019). *Klimatologi Pertanian*. Bandar Lampung: Pusaka Media.

Wu, Q. (2024). Sharing Work in Earth Engine: Basic UI and Apps. In J. A. Cardille, M. A. Crowley, D. Saah, & N. E. Clinton (Eds.), *Cloud-Based Remote Sensing with Google Earth Engine* (pp. 603–627). Cham: Springer International Publishing. Retrieved July 25, 2025, from https://link.springer.com/10.1007/978-3-031-26588-4_30

Yanuarsyah, I., Susetyo, B., Hermawan, E., & Hudjimartsu, A. S. (2025). *PENGANTAR GEOINFORMATIKA*. Padang: Gemilang Press Indonesia.

Yengoh, G. T., Dent, D., Olsson, L., Tengberg, A. E., & Tucker III, C. J. (2016). *Use of the Normalized Difference Vegetation Index (NDVI) to Assess Land Degradation at Multiple Scales*. SpringerBriefs in Environmental Science. Cham: Springer International Publishing. Retrieved from http://link.springer.com/10.1007/978-3-319-24112-8

Zhang, H., Zhang, F., Ye, M., Che, T., & Zhang, G. (2016). Estimating daily air temperatures over the Tibetan Plateau by dynamically integrating MODIS LST data. *Journal of Geophysical Research: Atmospheres*, *121*(19), 11425–11441. Wiley-Blackwell. Retrieved July 25, 2025, from https://doi.org/10.1002/2016JD025154